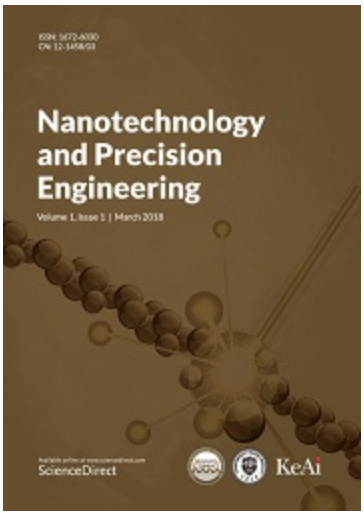

Enhancement of surface wettability via micro and nanostructures by single point diamond turning

Journal:	*Nanotechnology and Precision Engineering*
Manuscript ID	NPEE-2019-0004.R1
Manuscript Type:	Nano Fabrication and Metrology
Keywords:	contact angle, wettability, single point diamond turning, hydrophobicity, structured surface

SCHOLARONE™
Manuscripts

Enhancement of Surface Wettability via Micro- and Nanostructures by single point diamond turning

Nicolás Cabezudo[1], Jining Sun[1*], Behnam Andi[1], Fei Ding[2], Ding Wang[3], Wenlong Chang[2], Xichun Luo[2], Ben B Xu[3],

[1] School of Engineering and Physical Sciences, Heriot-Watt University, Edinburgh, UK

[2] Centre for Precision Manufacturing, DMEM, University of Strathclyde, Glasgow, UK

[3] Faculty of Engineering and Environment, Northumbria University, Newcastle upon Tyne, UK

*Jining.Sun@hw.ac.uk

For Review Only

Abstract

Studies on surface wettability have received tremendous interest due to their potential applications in research and industrial processes. One of the strategies to tune surface wettability is modifying surface topography at micro- and nanoscales. In this research, periodic micro- and nanostructures were patterned on several polymer surfaces by ultra-precision single point diamond turning to investigate the relationships between surface topographies at the micro- and nanoscales and their surface wettability. This research revealed that single-point diamond turning could be used to enhance the wettability of a variety of polymers, including polyvinyl chloride (PVC), polyethylene 1000 (PE1000), polypropylene copolymer (PP), and polytetrafluoroethylene (PFTE), which cannot be processed by conventional semiconductor-based manufacturing processes. Materials exhibiting common wettability properties ($\theta \approx 90°$) changed to exhibit "superhydrophobic" behavior ($\theta > 150°$). Compared with the size of the structures, the aspect ratio of the void space between micro- and nanostructures has a strong impact on surface wettability.

Key words: contact angle, wettability, single-point diamond turning, structured surface, hydrophobicity.

Background

Surface behavior plays a key role in many physical or chemical properties such as wettability [1], optical properties [2], thermal emissivity [3], corrosion [4], and other biological and chemical processes [5-8]. Wettability is the tendency of one fluid to

spread on or adhere to a solid surface. Wettability can be measured by the contact angle, which is conventionally measured through the liquid, where a liquid–vapor interface meets a solid surface. Different theories have been proposed to explain wetting phenomena [9]. Young defined the wettability for ideal surfaces as in Equation (1).

$$\cos(\theta_{ideal}) = \frac{\Upsilon_{sv} + \Upsilon_{sl}}{\Upsilon_{lv}} \quad (1)$$

where θ is the ideal contact angle, γ_{lv} is the surface tension of the liquid/vapor interface, γ_{sl} is the surface tension of the solid/liquid interface, and γ_{sv} represents the surface tension of the solid/vapor interface. Depending on the value of the contact angle, surfaces can be classified into four groups: superhydrophobic (θ > 150°), hydrophobic (90° < θ < 150°), hydrophilic (10° < θ < 90°), and superhydrophilic (θ < 10°) [10].

The wettability can also be researched by the advancing contact angle (θ_a), receding contact angle (θ_r), and hysteresis angle (θ_H). The advancing contact angle is a measure of the liquid–solid cohesion, whereas the receding contact angle is a measure of liquid–solid adhesion. Contact angle hysteresis can arise from molecular interactions between the liquid and solid or from surface anomalies, such as roughness or heterogeneities [11]. It is defined as the difference between the value of the angle of advance and the value of the receding contact angle (Equation (2)).

$$\theta_H = \theta_A - \theta_r \quad (2)$$

Surface energy and topography are the main factors affecting wettability. Wettability has been widely researched as a function of surface texture, material's chemistry, and processing conditions [12].

Surface topography can be altered modifying roughness [13,14]. The presence of features on surfaces can lead to large values of hysteresis where substantial forces may be required to initiate drop movement [15]. For very rough surfaces, drops can be suspended atop patterns, leaving air between them [16]. This suspension enables to have substrates with superhydrophobic behavior where drops can roll easily on them behaving as self-cleaning surfaces.

For Review Only

Wenzel and Cassie–Baxter created models for explaining wettability in real surfaces that exhibit some degree of roughness or are chemically heterogeneous. The Wenzel model supposes that a liquid can penetrate in the pores of the surface, and contact is homogeneous. Wenzel's equation is shown in Equation (3):

$$\cos(\theta_W) = \mathrm{r} \bullet \cos\theta_{ideal} \quad (3)$$

where θ_{ideal} is the contact angle in an ideal surface that cannot be practically obtained. θ_W is the contact angle in a real surface, and r is the Wenzel roughness factor. The factor r tries to explain that the roughness enhances the wettability properties of the smooth surfaces.

The Cassie–Baxter model describes heterogeneous wetting contact between the droplet and surface due to air entrapment. According to this theory, there is an area fraction where the liquid and solid are in contact and another area fraction where the liquid and gas stay in contact. The Cassie–Baxter model is defined in Equation (4).

$$cos(\theta_{CB}) = f_1 \bullet cos\,\theta_1 + f_2 \bullet cos\,\theta_2 \quad (4)$$

where θ_{CB} is the contact angle in a real surface, θ_1 and θ_2 are the contact angles of the two surfaces that are in contact (liquid–vapor and liquid–solid), and f_1 and f_2 are the apparent area fractions of surface components. Sketches of the Wenzel and Cassie–Baxter model are shown in Figure 1.

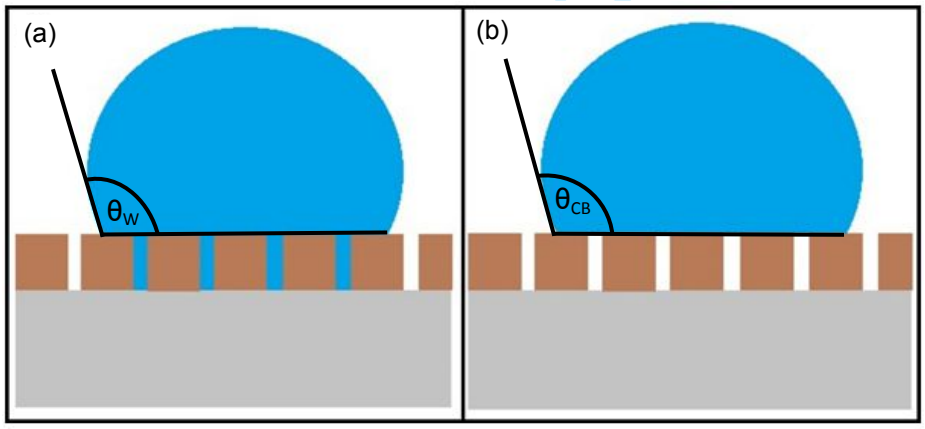

Figure 1- Sketches of a liquid droplet in (a) the Wenzel state with an apparent contact angle θ_W and (b) the Cassie–Baxter state with an apparent contact angle $\theta_{CB.}$

The contact angle is generally expected to obey the Wenzel model on substrates with moderate roughness, and it follows Cassie–Baxter behavior on highly rough surfaces. On hydrophobic surfaces ($\theta \approx 100^o$) of moderate roughness ($r_s \approx 2$), both Wenzel and

Cassie–Baxter states can co-exist. Some researchers believe the wettability models are limited because they use contour area rather than the contact line [17].

Superhydrophobic examples are found in lotus leaves [18] and certain insects and birds [19] where superhydrophobicity is achieved by surface textures consisting of micro- and nano-scale hierarchical structures. On the basis of these principles, two main strategies are developed for the preparation of superhydrophobic surfaces. One strategy consists of the deposition of hydrophobic materials that can be applied as coating layers such as poly(dimethylsiloxane) (PDMS) [20] or fluorinated silane compounds [21]. This strategy is associated with certain disadvantages such as cost, long procedure, and problems with substrate biocompatibility. The other strategy consists of machining of patterns on the surfaces by photolithography and electron beam lithography [22]. Photolithography has the disadvantage of limited choices in photoresist and substrate. Electron beam lithography presents the disadvantage of being a slow and expensive manufacturing technique that cannot be applied at a large scale.

Single point diamond turning (SPDT) is a versatile and highly controllable technique for manufacturing micro- and nanostructured surfaces with high accuracy. Compared with lithography technologies, SPDT can be used to machine a wide range of materials including polymers, metals, and ceramics, with high throughput at very large scales. This technique is based on turning with diamond as the cutting tool to mechanically remove materials with a precision in several nanometers on a wide variety of materials. SPDT is affected by process and material factors. The material factors include material swelling and recovery, grain boundaries, material spring back, and minimum undeformed chip thickness [23].

Through manufacturing of micro- and nanostructures on a variety of materials by SPDT, this research aimed to investigate how surface topographies affect wettability in hydrophobic and hydrophilic regimes. For this reason, micro- and nanostructures on the surfaces of several materials, including aluminum, polyvinyl chloride (PVC), polyethylene, polypropylene copolymer, PFTE, and polypropylene copolymer (PP), with feature dimensions from 500 nm to several micrometers, were employed. The surface of the different patterned areas and the wettability of these materials were characterized and analyzed. Finally, the values of contact angles obtained for the different patterned and flat surfaces were compared, and the patterns' height was found to affect the wettability for these materials.

For Review Only

Experimental Procedures

Through a customized five axis ultra-precision machine, micro- and nanogratings (500 nm, 1 μm, 2 μm, and 4 μm) were machined on materials including aluminum, PVC, polyethylene 1000 (PE 1000), polyethylene 500 (PE 500), polypropylene copolymer (PP), and PFTE. Under a spindle speed of 1000 rpm, feed rates of 4 mm/min, 2 mm/min, 1 mm/min, and 0.5 mm/min were employed to achieve 4 μm, 2 μm, 1 μm, and 0.5 μm per revolution. A sharp point diamond tool with an inclined angle of 53° was used. The size of the structures was controlled by changing the cutting depth. The 53º inclined angle ensured that the width of the gratings was the same as the cutting depth. Mineral spirit mist was used as coolant during the cutting process. To ensure the consistency of the cutting process, all substrates (75 mm x 25 mm) were mounted circularly around the center of the headstock (Figure 2(a)). An optical microscope image of the diamond cutting process is shown in Figure 2(b). On each substrate, gratings in dimensions of 4 μm, 2 μm, 1 μm, and 0.5 μm were cut within the ribbon areas 1–4 (Figure 2(c)). The fabrication results were measured by scanning electron microscopy (SEM; FEI Quanta 3D FEG). To avoid contaminating the surfaces, all samples were uncoated and measured under low vacuum SEM mode (120 Pa).

The wettability of the surfaces was characterized by a measuring the contact angles (Krüss Drop Shape Analyzer – DSA30) at different areas of each sample, along vertical and parallel directions (Figure 2(c)). To reduce error in measurement, five water droplets (2 μL each) were randomly placed in each area. For each droplet, apparent contact angles including static contact angle, advancing contact angle, and receding contact angle were measured, and the average value was considered the measurement result.

For Review Only

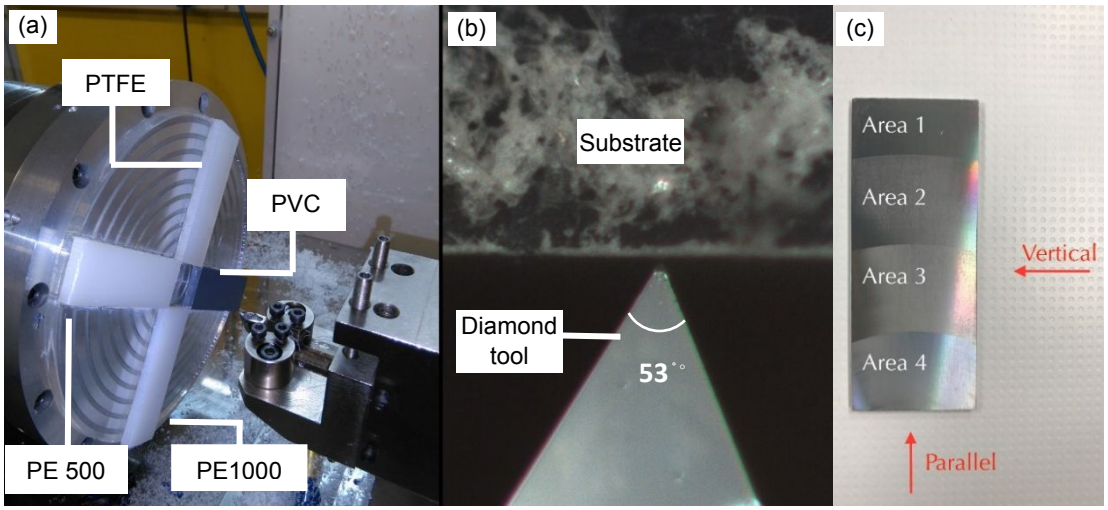

Figure 2 Overall manufacturing process. (a) Experimental setup of diamond turning process; (b) microscope image of the diamond cutting process; (c) an Al sample with four different structures in 4 μm (Area 1), 2 μm (Area 2), 1 μm (Area 3), and 500 nm (Area 4).

Results and Discussion

SEM images of the micro and nanostructures from 4 μm to 500 nm on different substrates are shown in Figure 3. Under the same cutting depth, the actual surface topography of the gratings on metal and plastic surfaces slightly differed due to the different elastic recovery rates after material removal.

For each material, contact angles on flat surface and structured surfaces (areas 1–4) were measured. The measurement results for contact angles are shown in Figures 4–9. For Al and PVC, all contact angles were measured along both vertical and parallel directions (Figure 2(c)). The measurement results for these two materials are illustrated in Figures 4 and 5.

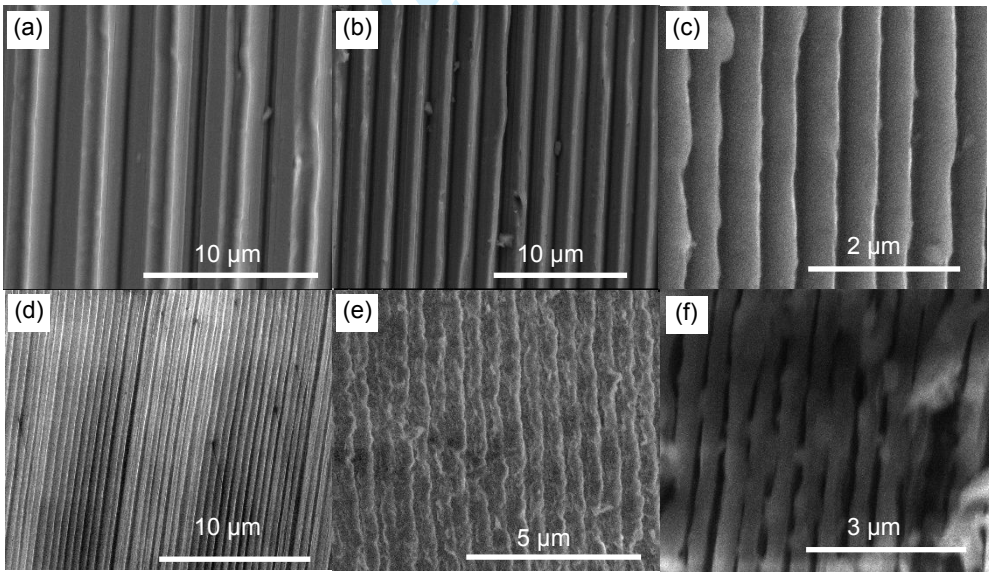

Figure 3 – SEM images of micro and nanostructures on different materials: (a) 4 μm gratings on Al; (b) 2 μm gratings on Al; (c) 0.5 μm gratings on Al; (d) 0.5 μm gratings on PE1000; (e) 0.5 μm gratings on PTFE; and (f) 0.5 μm gratings on PVC.

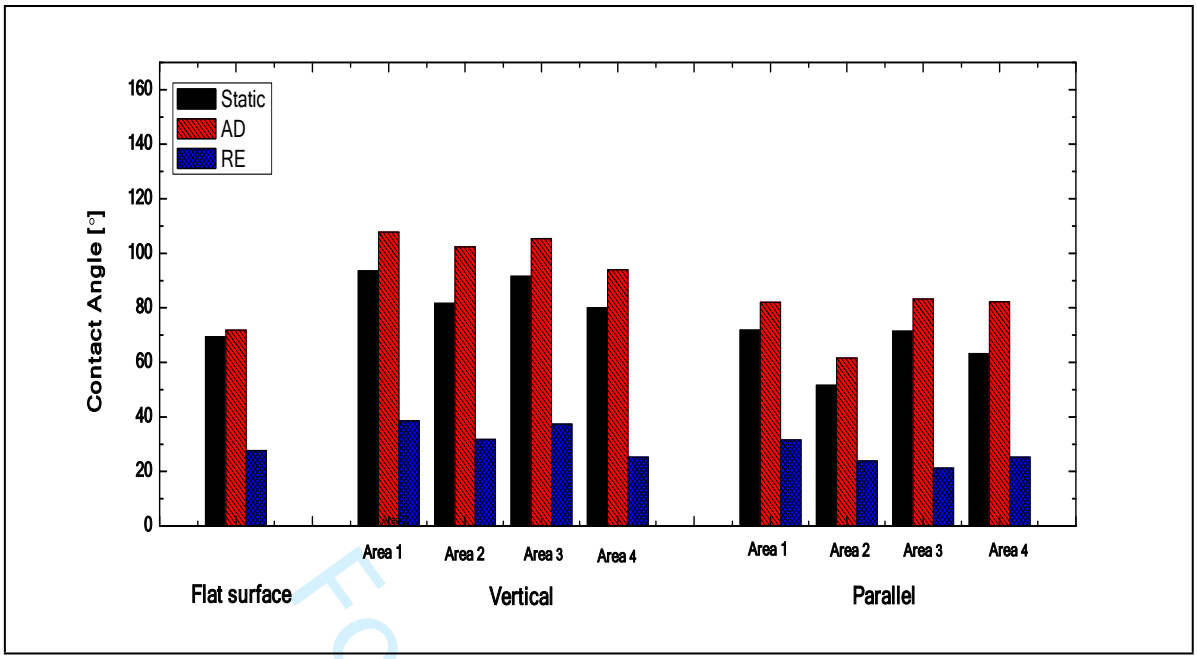

Figure 3 - Contact angle measurements for aluminum.

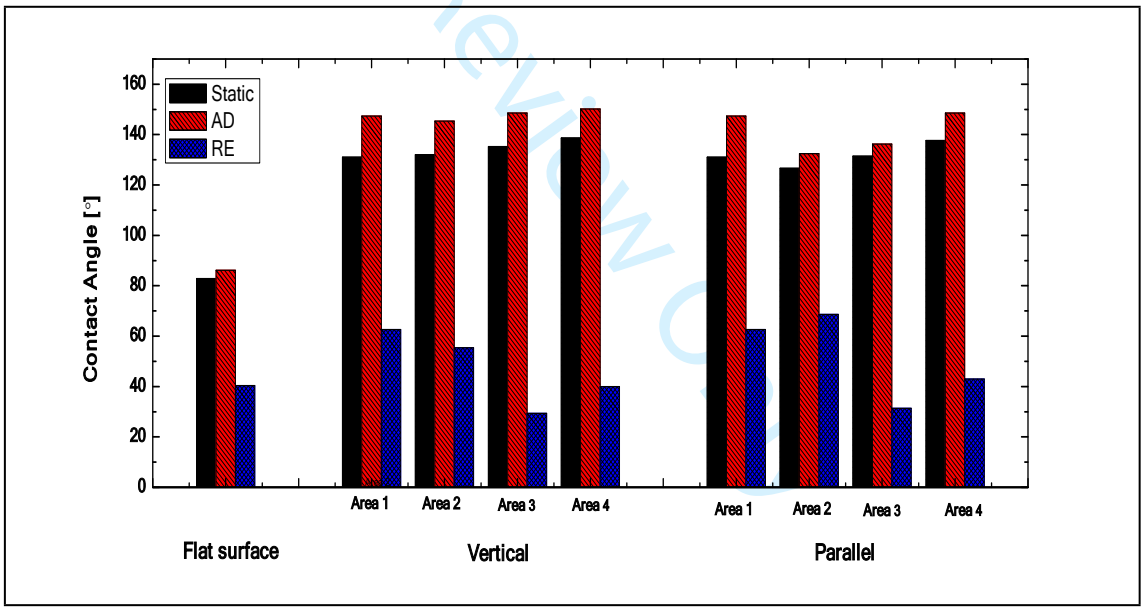

Figure 5 - Contact angle measurements for PVC.

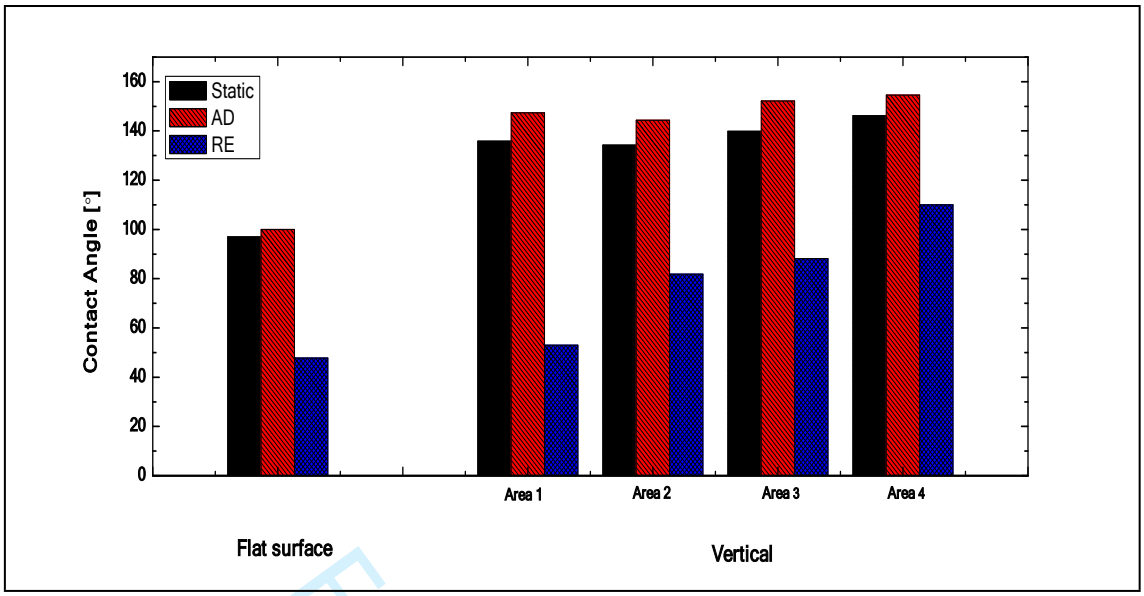

Figure 6 - Contact angle measurements for PE 1000.

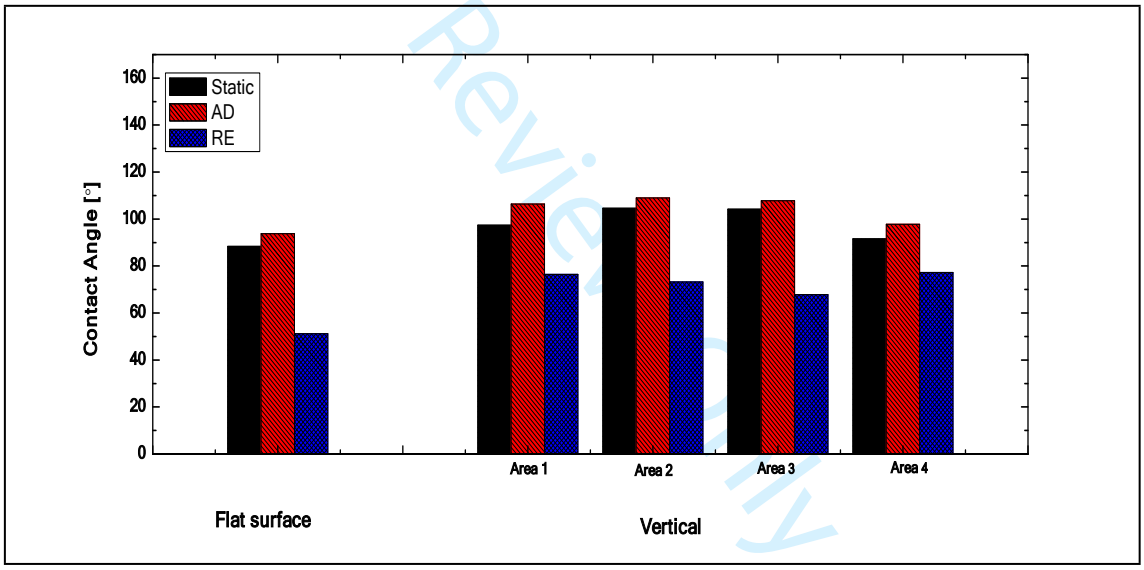

Figure 7 - Contact angle measurements for PE 500.

For Review Only

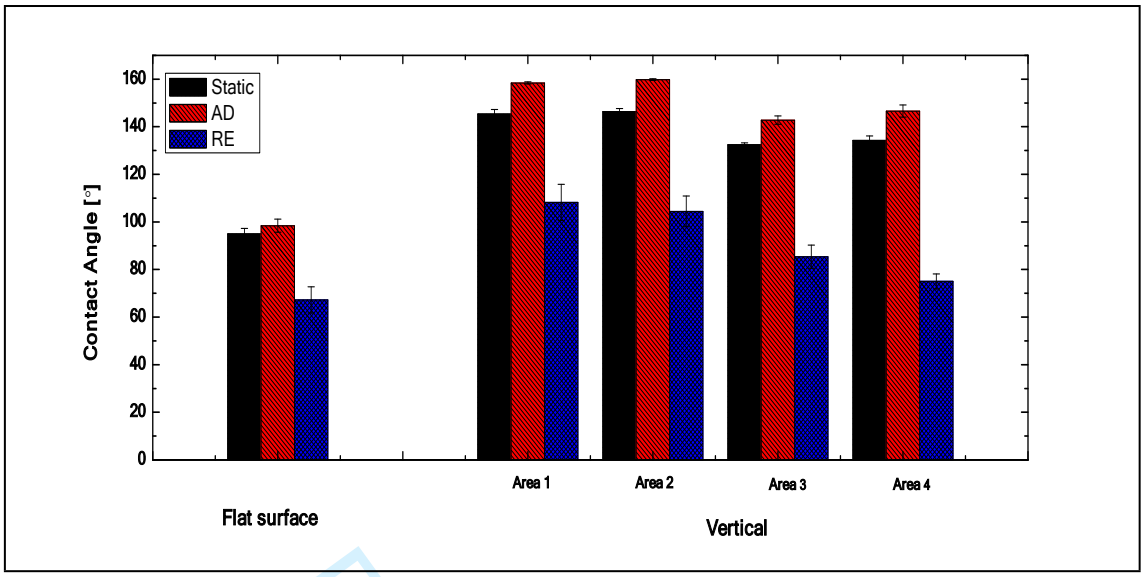

Figure 8 - Contact angle measurements for PP.

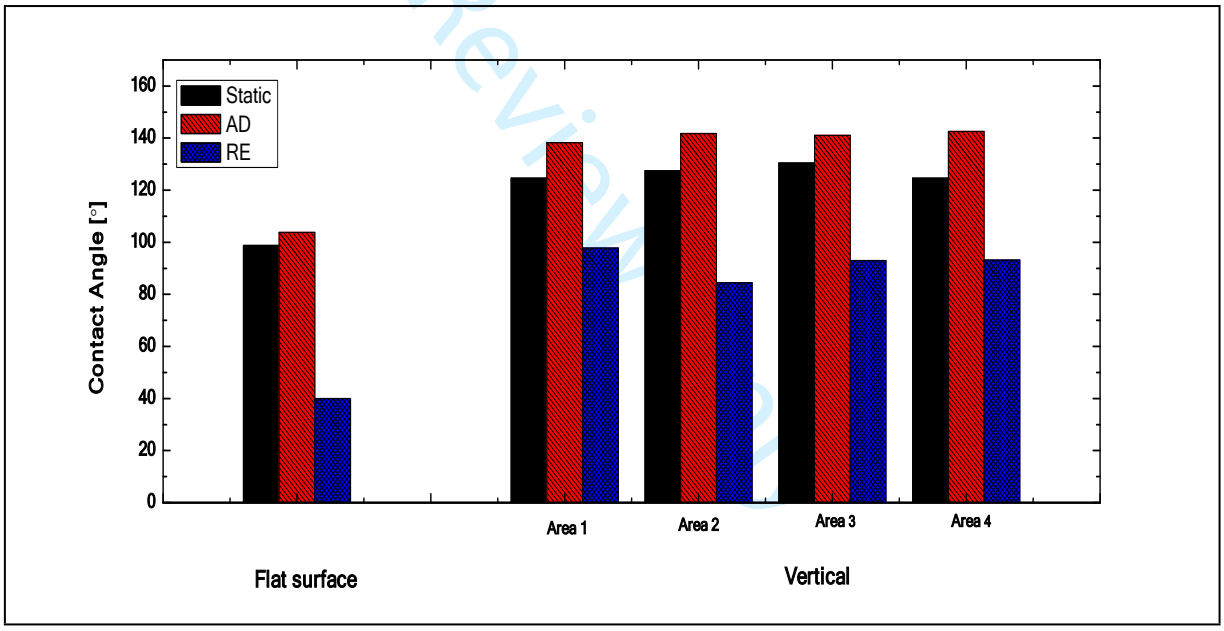

Figure 9 - Contact angle measurements for PTFE

For each material, the roughness factor (R_f) and packing parameter (p) was calculated. The packing parameter is the fraction of the structured surface area over the total area of the substrate. The roughness factor was estimated theoretically given that the patterns adopt a square shape and considering the height, width, and distance. For the different patterned areas, the distance between patterns was constant, so pitch distance did not influence the roughness factor. The width of the patterns showed small

variations in the different materials due to the different elastic behavior of the materials during the machining process, resulting in minimal changes in the roughness factor. Therefore, the roughness factor would depend mainly on the height of the patterns. Considering that the height of the pattern ranged from 4 μm to 500 nm, the roughness factor was expected to decrease from area 1 (pattern height of 4 μm) to area 4 (pattern height of 500 nm). The roughness factors and packing parameters for different materials are shown in Table 1.

Table 1 – Roughness factor and packing parameter estimation for the different materials.

Material	R_f	p
Aluminum	3.8 – 4.79	0.84 – 0.90
PVC	3.9 – 5.08	0.55 – 0.96
PE 1000	3.83 – 4.56	0.76 – 0.79
PE 500	3.01 – 4.07	0.54 – 0.73
PTFE	1.08 – 2.86	0.76 – 0.80
PP	2.62 – 4.12	0.70 – 0.76

Given the existence of micro and nanostructures, in areas 1 and 3, the wettability of aluminum changed from hydrophilic (θ = 69.4º) to hydrophobic (up to 93.6º). This result contradicts the Wenzel model defined in Equation (3). The Wenzel model predicts that an increase in the surface roughness for hydrophilic materials can enhance their hydrophobicity behavior and exhibit small apparent contact angles. Thus, air bubbles successfully trapped by these structures possibly affect the wetting behavior of aluminum substrates, and the droplet follows a composite state. If the droplet is in the composite state, the apparent contact angle should be calculated using Cassie and Baxter's model defined by Equation (4). *Zu et al.* performed a theoretical analysis on substrates patterned by square patterns following the Cassie–Baxter model. This model predicts that the area fraction of the solid–liquid interface, *f*, is only dependent on the pattern width and pitch distance. This model predicts that the apparent contact angle should decrease with the increase in pattern height for flat substrates with θ < 90º [24]. This model cannot explain the experimental results. These results can be explained by taking into account the phenomenon of passivation where aluminum forms a thin surface layer of aluminum oxide upon contact with oxygen in the atmosphere through oxidation, which is enhanced at high temperatures. This layer creates porosity on the surface of the structures. The formation of this oxidized

For Review Only

structure can resemble anodized aluminum. The surface of passivated aluminum transitions from slightly hydrophilic to moderately hydrophobic up to film thicknesses of about 6 μm [25].

PVC, PE 1000, PP, and PTFE exhibited a great change in their wettability behavior ($\Delta\theta > 50^{\circ}$) when micro- and nanostructures were introduced to the surfaces, shifting from non-extraordinary wettability behavior ($\theta \approx 90^{\circ}$) to superhydrophobic behavior ($\theta > 150^{\circ}$). All four areas with structures ranging from 500 nm to 4 μm showed similar contact angles. The Wenzel model predicts that patterned materials with intrinsic contact angles $\theta > 90^{\circ}$ demonstrate an enhancement in their hydrophobic behavior when the roughness factor is increased. According to *Nosonovsky et al.*, the change in contact angle in the Wenzel model depends on the different geometric parameters of the surface structure such as width and height of the pillars, distance between pillars, patterns shape, and pattern packing [26]. This model explains that the aspect ratio and packing parameter of the structures have an outstanding effect on the variation in the contact angle on surfaces with patterned structures. In the different patterned areas, the pattern height decreased from 4 μm to 500 nm, whereas the width of the patterns showed small variations in the different materials due to the different elastic behavior of the materials during the machining process. The aspect ratio was in the range of 1–5 for the different manufactured areas. In the different patterned surfaces, p oscillated between 0.5 and 0.9. According to this theoretical analysis, an increase in the aspect ratio for materials with intrinsic contact angles $\theta > 90^{\circ}$ could extensively enhance the hydrophobicity of the materials.

With the patterned surfaces, the hydrophobicity of PE 500 only slightly increased ($\Delta\theta \approx 10^{\circ}$–$15^{\circ}$). According to theoretical analysis, the Cassie–Baxter model indicates that the height of the pillars does not influence the wettability of the materials [24]. This phenomenon is quite unique especially when compared with PE 1000, which has very similar wettability on flat surfaces. This effect can also be explained by their different surface topography. PE 1000 offers higher wear resistance and impact strength than PE 500. Therefore, under the same cutting parameters, PE1000 is more difficult to remove than PE 500. As shown in Figure 10, the gaps between each patterns (1 μm) on PE 1000 (Figure 10(a)) were smaller than those on PE 500 (Figure 10(b)), leading to a void space with high aspect ratio, which facilitated air trapping and resulted in a high contact angle. Thus, for hydrophobic surfaces ($\theta \approx 100^{\circ}$) of moderate roughness ($R_s \approx 2$), both wettability models can co-exist, and the droplet may stay in a state of metastable equilibrium [24].

https://mc03.manuscriptcentral.com/npe

For Review Only

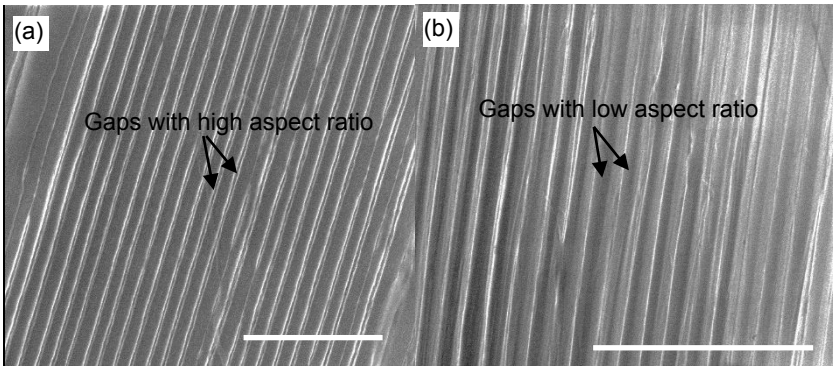

Figure 10. SEM images of 1 μm gratings on PE 1000 (a) and PE 500 (b). (Scale bar is 10 μm).

The contact angle hysteresis of each material is also studied. Theoretical analysis of other researchers demonstrated that contact angle hysteresis depends on the ratio width of the structures / pitch between the structures, as well as the density of the pillars [27,28]. Among the tested materials, Al, PE 500, PP, and PTFE did not show a measurable change in contact angle hysteresis with the different patterns, whereas PE 1000 exhibited an enhancement in contact angle hysteresis with an increased the roughness factor. By contrast, PVC showed a reduction in contact angle hysteresis when the roughness factor increased. Our observation revealed a relationship between contact angle hysteresis and the size of the surface structures. Recent research demonstrated that contact angle hysteresis is strongly correlated with the projected area fraction for fully wetting space (f_w) [29]. For all the polymer materials used in this work, f_w varied from 0 to 1, depending on the structures and surface finish. Although the same size of structures was achieved on different materials, the surface finish differed (Figure 3). Such a difference caused the unpredictable behavior of contact angle hysteresis on different materials. Other studies indicated that contact angle hysteresis is affected by the height of the patterns, pitch distance [30], and shape of patterns [31, 32]. The main finding in the literature is that sharp patterns lead to a remarkable enhancement in contact angle hysteresis [33]. Further research should focus on controlling surface finish and the shape of structures for an in-depth study of contact angle hysteresis.

Conclusions

By using SPDT, this research demonstrated the changes in surface wettability through micro- and nanostructures on materials that cannot be processed by conventional

https://mc03.manuscriptcentral.com/npe

lithography-based technologies. Results revealed that the wettability of polymers such as PVC, PE 1000, PP, and PTFE can be greatly enhanced ($\Delta\theta \approx 50^{o}$). Meanwhile, aluminum and PE 500 exhibit a moderate change in their wettability properties ($\Delta\theta \approx 10^{o}$) when features are manufactured on their surfaces. From 500 nm to 4 μm, the correlation between the sizes of the structures and surface wettability is not strong. In such a scale, the aspect ratio of void structures plays an important role in surface wettability. For the same material, void space with high aspect ratio can trap air easily, resulting in a high contact angle. In addition, the experimental results can be well explained through the introduction of the roughness factor and the packing parameter, which indicates that surfaces with different wettabilities can be tuned through these parameters and then fabricated by SPDT.

For Review Only

Acknowledgment

The authors gratefully acknowledge the financial support from Heriot-Watt University (Edinburgh) and the EPSRC (EP/K018345/1) for this study.

References

[1] De Gennes P.G., *Wetting: statics and dynamics*, Reviews of Modern Physics. **57**, (3) 827–863, (1985).

[2] DeAro J. A., Weston K. D., Buratto S. K., Lemmer U., *Mesoscale optical properties of conjugated polymers probed by near-field scanning optical microscopy*, Chem. Phys. Lett. **277**, 532-538 (1997).

[3] Wang L., Xu G., Liu C., Hou H., Tan S., *Surface-modified CeO_2 coating with excellent thermal shock resistance performance and low infrared emissivity at high-temperature*, Surface and Coatings Technology **357**, 559-566 (2019).

[4] Manam N.S., Harun W.S.W., Shri D.N.A., Ghani S.A.C., Kurniawan T., Ismail M.H., Ibrahim M.H.I., *Study of corrosion in biocompatible metals for implants: A review*, Journal of Alloys and Compounds **701**, 698-715 (2017).

[5] Garrett T.R., Bhakoo M., Zhanga Z., Bacterial adhesion and biofilms on surfaces, Progress in Natural Science **18**, Issue 9, 1049-1056 (2008).

[6] Anselme K., Ponche A., Bigerelle M., *Relative influence of surface topography and surface chemistry on cell response to bone implant materials. Part 2: Biological aspects*, SAGE Journals **224**, Issue 12, 1487-1507 (2010).

[7] Lundqvist M., Stigler J., Elia G., Lynch I., Cedervall T., *Dawson K.A., Nanoparticle size and surface properties determine the protein corona with possible implications for*

biological impacts, Proceedings of the National Academy of Sciences of the United States of America **105**, (38) 14265-14270 (2008).

[8] Albanese A., Tang P.S., Chan W.C.W., *The Effect of Nanoparticle Size, Shape, and Surface Chemistry on Biological Systems*, Annual Review of Biomedical Engineering **14**, 1-16 (2012).

[9] Loeb G.I., Schrader M.E., *Modern Approaches to Wettability: Theory and Applications*, Springer Science (1992).

[10] Mittal K. L., *Advances in Contact Angle, Wettability and Adhesion*, Wiley (2018).

[11] Extrand C. W., In *Encyclopedia of Surface and Colloid Science,* Marcel Dekker, 2414 (2002).

[12] Miwa M., *Effects of the Surface Roughness on Sliding Angles of Water Droplets on Superhydrophobic Surfaces*, Langmuir 16 (13), 5754–5760 (2000).

[13] Wenzel, R. N., *Resistance of solid surfaces to wetting by water*, Ind. Eng. Chem., **28** (8), 988–994 (1936).

[14] Cassie A. B. D., Baxter S., *Wettability of porous surfaces*, Trans. Faraday Soc. **40**, 546-551 (1944).

[15] Bartell, F. E.; Shepard, J. W. J., *Surface Roughness as Related to Hysteresis of Contact Angles. II. The Systems Paraffin–3 Molar Calcium Chloride Solution–Air and Paraffin–Glycerol–Air*, Phys. Chem., **57**, 455-458 (1953).

[16] Johnson, R. E., Jr.; Dettre, R. H., Jhonson JR., *Contact Angle Measurements on Rough Surfaces*, Advances in Chemistry **43**, (8), 136–144 (1964).

[17] Gao L. C., McCarthy T. J., *How Wenzel and Cassie were wrong*, Langmuir **23**, 3762-3765 (2007).

[18] Quéré D., *Rough ideas on wetting*, Physica A: Statistical Mechanics and its Applications **313** (1-2), 32-46 (2002).

[19] W. Barthlott and C. Neinhuis, *Purity of the sacred lotus, or escape from contamination in biological surfaces*, Planta **202**, 1-8 (1997).

[20] M. T. Khorasani, H. Mirzadeh and Z. Kermani, *Wettability of porous polydimethylsiloxane surface: morphology study*, Appl. Surf. Sci. **242**, (3), 339-345 (2005).

[21] X. Y. Song, J. Zhai, Y. L. Wang and L. Jiang, *Fabrication of Superhydrophobic Surfaces by Self-Assembly and Their Water-Adhesion Properties*, J. Phys. Chem. B **109**, 4048-4052 (2005).

[22] Lasagni F.A., *Fabrication and characterization in the micro-nano range new trends for two and three dimensional structures*, Springer (2011).

For Review Only

[23] Sohn A, Lamonds L, Garrard K. *Modelling of vibration in single-point diamond turning*, Proceedings of the ASPE, American Society for Precision Engineering, 21st annual meeting, (2006).

[24] Zu Q., Yan Y., Li J.,Han Z., *Wetting Behaviours of a Single Droplet on Biomimetic Micro Structured Surfaces*, Journal of Bionic Engineering **7**, 191–198 (2010).

[25] Buijnsters J., Surface Wettability of Macroporous Anodized Aluminum Oxide, ACS Appl. Mater. Interfaces 5 (8), 3224–3233 (2013).

[26] Nosonovsky M., Bhushan B., *Roughness-induced superhydrophobicity: a way to design non-adhesive surfaces*, J. Physics Condensed Matter **20**, 225009 (2008).

[27] Hejazi V., Nosonovsky M., *Contact angle hysteresis in multiphase systems*, Colloid Polym Sci **291**, 329 – 338 (2013).

[28] Shia Z., Zhan X., *Contact angle hysteresis analysis on superhydrophobic surface based on the design of channel and pillar models*, Materials & Design **131** 323–333 (2017).

[29] Cheng K., Naccarato B., Kim K.J, Kumar A., *Theoretical consideration of contact angle hysteresis using surface-energy-minimization methods*, International Journal of Heat and Mass Transfer **102**, 154–161 (2016).

[30] Forsberg P., *Contact Line Pinning on Microstructured Surfaces for Liquids in the Wenzel State*, Langmuir, **26** (2), 860–865 (2010).

[31] Eick J.D, Good R., Neumann A., *Thermodynamics of contact angles. II, Rough solid surfaces*, J Colloid Interfacial Sci, **53**, 235-238 (1975).

[32] Huh C., Mason S., *Effects of surface roughness on wetting (theoretical)*, J Colloid Interfacial Sci, 60, 11-38 (1977).

[33] Joanny J.F., Gennes P.G., *A model for contact angle hysteresis*, J. Chem. Phys. **81**, 552 (1984).

For Review Only